



SHARPENS YOUR THINKING

## Entropy-driven formation of the gyroid cubic phase

ELLISON, L. J., MICHEL, D. J., BARMES, F. and CLEAVER, D. J.

Available from Sheffield Hallam University Research Archive (SHURA) at:

<http://shura.shu.ac.uk/891/>

---

This document is the author deposited version. You are advised to consult the publisher's version if you wish to cite from it.

### Published version

ELLISON, L. J., MICHEL, D. J., BARMES, F. and CLEAVER, D. J. (2006). Entropy-driven formation of the gyroid cubic phase. *Physical review letters*, 97, p. 237801.

---

### Repository use policy

Copyright © and Moral Rights for the papers on this site are retained by the individual authors and/or other copyright owners. Users may download and/or print one copy of any article(s) in SHURA to facilitate their private study or for non-commercial research. You may not engage in further distribution of the material or use it for any profit-making activities or any commercial gain.

# Entropy-driven formation of the gyroid cubic phase

L.J. Ellison,<sup>1</sup> D.J. Michel,<sup>2</sup> F. Barmes,<sup>3</sup> and D.J. Cleaver<sup>1</sup>

<sup>1</sup>*Materials and Engineering Research Institute, Sheffield Hallam University, Sheffield S1 1WB, United Kingdom.*

<sup>2</sup>*Max Planck Institute for Biophysical Chemistry, Am Fassberg 11, D-37077 Göttingen, Germany.*

<sup>3</sup>*Centre Européen de Calcul Atomique et Moléculaire, 46 allée d'Italie, 69007 Lyon, France.*

(Dated: October 11, 2006)

We show, by computer simulation, that tapered or pear-shaped particles, interacting through purely repulsive interactions, can freely self-assemble to form the three-dimensionally periodic, gyroid cubic phase. The Ia3d gyroid cubic phase is formed by these particles both on compression of an isotropic configuration and on expansion of a smectic A bilayer arrangement. For the latter case, it is possible to identify the steps by which the topological transformation from non-intersecting planes to fully interpenetrating, periodic networks takes place.

PACS numbers: 61.20.Ja, 64.70.Nd, 61.30.-v

Non-spherical particles with purely repulsive interactions are known to form a number of phases intermediate between the isotropic fluid and crystalline solid states. In the 1980's, computer simulations of hard prolate particles [1] confirmed Onsager's classic prediction [2] that particle shape anisotropy can be a sufficient condition to induce the long-range orientational order found in nematic liquid crystals. Subsequently, hard spherocylinders were shown to form a smectic phase [3], while hard oblate particle systems were found to exhibit both discotic nematic [4] and cubatic order [5].

The phase properties of systems with purely steric interactions are important from a statistical mechanical perspective because the potential energy,  $U$ , of a steric system is, by definition, constant. Consequently, the Helmholtz free energy  $F = U - TS$  in the constant  $NVT$  ensemble is controlled by entropy alone and all phase transitions are entropy driven [6]. The concept of ordered phases forming due to entropic effects is counter-intuitive, since entropy is generally associated with disorder. Deeper examination of the transitions noted above shows, however, that they occur when, for example, the global system entropy can be enhanced by the sacrifice of some degree of "local" disorder. As well as defining entropy-driven transitions, studies of hard particle systems also closely inform aspects of the experimental behaviour of colloidal suspensions.

In this letter, we extend the range of phases accessible to purely repulsive objects by showing that tapered or pear-shaped particles can freely self-assemble to form the 3d periodic gyroid cubic phase. Due to their complexity and the supramolecular length-scales of their periodicities, very few particle-based simulations of cubic phases have been performed. The most convincing of these is Marrink and Tieleman's molecular dynamics (MD) study of glycerolmonoolein molecules organised in a diamond cubic structure [7]. Here, however, the cubic arrangement had to be preconstructed and weak constraints imposed to maintain the structure; without these, this system slowly converted into an inverted hexagonal arrangement [8]. Simulation has also been used to probe the rheological properties of the gyroid phase [9]. Here, though, so as to make hydrodynamic behaviour accessible, it was necessary to employ a phenomenological Lattice-Boltzmann description which offered no link to the nature of the underlying particles.

The objects considered here are described by the parametric hard Gaussian overlap (PHGO) approximation to Bézier-curve representations of cylindrically symmetric, tapered objects [10]. The PHGO approach makes it possible to simulate these non-centrosymmetric particles as single-site objects, with little computational overhead beyond that required for conventional ellipsoidal Gaussian overlap particles. As a result, multi-million-step simulation runs on 10,000 particle systems are readily achievable.

The underlying tenet of the PHGO model is that a convex object, such as a pear-shaped particle, can locally be well approximated by an ellipsoid, the appropriate ellipsoid being dependant on the direction from which the convex object is viewed. In the PHGO model, this approach is implemented by giving the effective ellipsoid lengths and breadths parametric dependence on the relative positions and orientations of the particles involved. As detailed in

ref [10] the PHGO contact function for two particles  $i$  and  $j$  is then expressed as:

$$\sigma(\hat{\mathbf{u}}_i, \hat{\mathbf{u}}_j, \hat{\mathbf{r}}_{ij}) = \sigma_0 \left[ 1 - \chi \left\{ \frac{\alpha^2 (\hat{\mathbf{r}}_{ij} \cdot \hat{\mathbf{u}}_i)^2 + \alpha^{-2} (\hat{\mathbf{r}}_{ij} \cdot \hat{\mathbf{u}}_j) - 2\chi (\hat{\mathbf{r}}_{ij} \cdot \hat{\mathbf{u}}_i) (\hat{\mathbf{r}}_{ij} \cdot \hat{\mathbf{u}}_j) (\hat{\mathbf{u}}_i \cdot \hat{\mathbf{u}}_j)}{1 - \chi^2 (\hat{\mathbf{u}}_i \cdot \hat{\mathbf{u}}_j)^2} \right\} \right]^{-\frac{1}{2}} \quad (1)$$

where

$$\sigma_0 = \sqrt{\frac{d_i^2 + d_j^2}{2}} \quad (2)$$

$$\alpha^2 = \left[ \frac{(l_i^2 - d_i^2)(l_j^2 + d_j^2)}{(l_j^2 - d_j^2)(l_i^2 + d_i^2)} \right]^{\frac{1}{2}} \quad (3)$$

$$\chi = \left[ \frac{(l_i^2 - d_i^2)(l_j^2 - d_j^2)}{(l_j^2 + d_j^2)(l_i^2 + d_i^2)} \right]^{\frac{1}{2}}. \quad (4)$$

Here,  $\hat{\mathbf{u}}_i$  is the unit orientation vector of particle  $i$  and  $\hat{\mathbf{r}}_{ij}$  is the inter-particle unit vector.  $l_i$  and  $d_i$  are the instantaneous length and breadth values associated with particle  $i$ . For tapered particles, these are effectively expressed as power series expansions in the dot product  $(\hat{\mathbf{r}}_{ij} \cdot \hat{\mathbf{u}}_i)$ . Thus,

$$d_i(\hat{\mathbf{r}}_{ij} \cdot \hat{\mathbf{u}}_i) = d_0 + d_1(\hat{\mathbf{r}}_{ij} \cdot \hat{\mathbf{u}}_i) + \dots + d_{10}(\hat{\mathbf{r}}_{ij} \cdot \hat{\mathbf{u}}_i)^{10} \quad (5)$$

$$l_i(\hat{\mathbf{r}}_{ij} \cdot \hat{\mathbf{u}}_i) = l_0 + l_1(\hat{\mathbf{r}}_{ij} \cdot \hat{\mathbf{u}}_i), \quad (6)$$

the coefficients being set to achieve the desired degree of particle tapering. The degree of tapering is characterized by a single parameter,  $k_\theta$ , which sets the locations of the Bézier control points that define the chosen particle shape [10]. The equivalent particle cone angle is then given by  $\arctan(1/k_\theta)$ . In this paper we show results obtained with particles like that shown in the inset to Fig 1b, characterized by the parameter values  $k = 3$ ,  $k_\theta = 3.8$ .

In a previous study we showed, by Monte Carlo (MC) simulation, that slightly tapered PHGO particles with a length to breadth ratio of  $k = 5$  form a bilayer smectic phase between the nematic and crystalline solid states [10]. Subsequent simulations using 1250 shorter ( $k = 3$ ) particles again found conventional liquid crystal phases for particles with either pronounced or mild degrees of taper. However, particles with intermediate tapering angles appeared to form a multi-domain curved bilayer state in which the particles developed locally well ordered bilayer patches, these being highly curved and randomly distributed throughout the simulation box.

By extending these simulations to system sizes of  $\simeq 10,000$ , we have now found that these moderately tapered particles actually spontaneously self-assemble to form a supramolecular 3d periodic arrangement (Figs 1). Further analysis of this structure shows it to be the Ia3d gyroid cubic phase. This can be seen from Fig 1b, which shows the two interpenetrating networks of channels and triply bonded nodes that characterise this phase. This network image was constructed by performing a cluster analysis based on the locations of the blunt ends of the individual tapered particles shown in Fig 1a and constructing 3d wireframe plots of the two independent networks identified by this analysis. We have obtained this periodic Ia3d structure both by compression of isotropic configurations and by expansion from an ordered crystal initial configuration through the intermediate smectic A bilayer phase.

For the system depicted in Figs 1, the Ia3d phase formed at number density  $\rho = 0.336$  on compression of an isotropic configuration and  $\rho = 0.350$  on expansion of a bilayer smectic. The planar smectic bilayer phase could not be regained from compression of the cubic phase, but the isotropic fluid phase *was* readily obtained on expansion of the Ia3d phase. The Ia3d phase shows a reasonably wide range of stability; we have obtained this structure for  $k = 3$  particles with  $3 \leq k_\theta \leq 4.4$ , corresponding to equivalent cone angles of between  $12.8^\circ$  and  $18.4^\circ$ . It is also formed by the  $k = 4$ ,  $k_\theta = 4$  system. These structures have been obtained from both MD simulations of a soft-repulsive version of the PHGO model and independent MC simulations of the hard version of the PHGO model. To allow commensurabilities between the Ia3d structure and the simulation box to develop naturally, box-shape variation moves were employed in both sets of simulations to ensure the isotropy of the pressure tensor. The long-time particle mobility determined from the MD simulations was isotropic and of the same order as that obtained in the neighbouring smectic A bilayer phase.

The Ia3d structure is well known in experimental studies of lyotropic liquid crystals [11] and block copolymers and its dividing surface, “the gyroid surface”, is one of the family of infinite periodic minimum surfaces [12]. Supramolecular cubic phases, including the Ia3d structure, have also been seen in studies of thermotropic cubic LC systems [13] based

on, e.g., polycatenar [14] and dendrimer [15] molecules. These are solvent-free systems based on highly functionalised molecules comprising flexible and rigid units arranged to promote a variety of molecule shapes (cone, rod+coil, shuttlecock, ...). Our simulations indicate, though, that particle shape alone is a sufficient condition to induce such behaviour.

It is interesting to relate this result to the copolymer and lyotropic systems traditionally associated with the gyroid phase. Generally, the transition from lamellar to gyroid structures is thought to be induced by the interfacial area available becoming large for the total system volume. In traditional gyroid-forming systems, it is relatively straightforward to relate this area to the concentrations and/or chemical compositions of the various components involved. In our repulsive pear systems, the relevant interface is the mid-surface of the curved bilayers apparent in Fig 1a. The area of this mid-surface is itself set by the particle shape and the extent to which the two leaflets interdigitate. The latter is not constrained, however, and has been found to vary with pressure [10]. The gyroid phase usually occupies a narrow region of stability sandwiched between lamellar and hexagonal regions. Like many experimental systems involving tapered (as opposed to wedge-like) dendrimers, however, the repulsive pear-shaped particles studied here do not appear to have a stable hexagonal phase.

Our findings also suggest potential routes towards the self-assembly of 3d periodic structures encompassing a broad range of length scales. Arranging dielectric scatterers on regular arrays is central to work examining photonic bandgap behaviour and has motivated studies of self-assembling nanoparticle systems. Our results suggest, however, that appropriate tuning of colloidal particle shape may be sufficient to induce such nanostructures to develop spontaneously. To this end, we note that continuum treatments of vesicle shape predict that pear-shaped objects can spontaneously develop under appropriate conditions [16] while recent work on colloidal particles with protrusions have shown that such objects can be produced reproducibly [17].

We have also used our MD simulations to examine the structural rearrangements associated with the formation of the Ia3d phase on expansion of a bilayer smectic phase to  $\rho = 0.350$ . The early stages of this are illustrated by the wireframe plots and particle-configuration schematics shown in Figs 2 and 3, respectively. Fig 2a shows a multiple bilayer arrangement adopted within a sub-region of our simulation box in the early stages of this run, the four planes indicating the locations of the blunt ends of the individual particles at timestep 100,000 (the shade (colour on-line) associated with each particle end at timestep 0 is conserved through the image sequence of Fig 2). This planar topology was maintained for the first 180,000 timesteps of the run. Over this time, significant in-plane and a small amount of out-of-plane migration of individual particles was observed. Out-of plane (or flip-flop) migration is apparent from the occasional spotting of the planes with the shades (colours on-line) of their neighbouring planes. Additionally, multi-particle distortions such as that shown in Fig 3a were seen, involving radially aligned arrangements centred on sub-clusters of particle blunt ends. The occasional formation of these local clusters, involving particles from *two neighbouring* bilayers, proved a crucial step in the development of the cubic arrangement. These distortions led to some regions in the bilayer planes being temporarily denuded of particle blunt ends; these correspond to “holes” in the wireframe planes, such as the one apparent in the second plane down in Fig 2a. At time-step 200,000, this precursor hole in the second plane was penetrated by a “stalk” linking the two neighbouring planes (Fig 2b). A schematic particle-configuration representation of this structure is shown in Fig 3b. From the shade (colour on-line) distribution seen along this initial stalk in Fig 2b, it is apparent that its formation involved significant material transfer from the neighbour planes; particles from the holed second plane only make up the very central section of the stalk.

Following this first stalk-formation event, further stalks developed (Fig 2c) and some stalk dissolution events also took place. While these processes proved very active, with the stalk arrangements morphing continuously, the instantaneous in-plane distributions of stalks and holes were generally hexagonal, as suggested in a previous experimental assessment of this transition [18]. By timestep 800,000 (Fig 2d), the original planar topology was significantly altered, with numerous stalks linking the remnants of the original planes. The considerable mixing of shades (colours on-line) seen in this Figure also indicates the extent of the particle migration exhibited throughout this structural rearrangement. In this simulation, the Ia3d structure of Fig 1a was fully formed by timestep 1,500,000, after which it remained essentially unaltered over several million further timesteps. While this structure remained fixed, we stress that particle mobility was maintained at its previous level as this simulation was run on. The mechanisms illustrated in Figs 2 show that each of the two interpenetrating but unconnected networks depicted in Fig 1b was, then, substantially developed from stacks of non adjacent planes (e.g. planes 1, 3, 5, ...) in an initial bilayer arrangement. This process was complicated somewhat, by the occasional transfer of particles between leaflets (e.g. by flip-flop) and by the formation of competing domains. However, the underlying mechanism we have observed here demonstrably follows the scheme proposed 15 years ago by Clerc et al when considering the topological changes involved in the transitions of their water + surfactant systems [19].

In summary, we have shown, by computer simulation, that hard and soft-repulsive pear-shaped particles spontaneously form the Ia3d gyroid cubic phase. The ability of these purely repulsive systems to form such a phase

represents an extension to the known range of entropy driven processes. It also raises the prospect that cubic phases may be accessible to suitably shaped aggregates or particles of any size from colloids upwards. By tracking particle configurations, we have also observed the mechanisms by which an initial smectic bilayer arrangement undergoes a topological rearrangement into the gyroid phase.

### Acknowledgements

The authors acknowledge useful conversations with Chris Care, Siewart-Jan Marrink, Volker Knecht and Claudio Zannoni. LJE thanks SHU for a PhD bursary and HPC Europa for funding a development visit to CINECA, Bologna.

- 
- [1] D. Frenkel, B.M. Mulder and J.P. McTague, *Phys. Rev. Lett.* **52**, 287 (1984)
  - [2] L. Onsager, *Ann. N.Y. Acad. Sci.* **51**, 627 (1949)
  - [3] J.A.C. Veerman and D. Frenkel, *Phys. Rev. A* **41**, 3237 (1990)
  - [4] D. Frenkel and B.M. Mulder, *Mol. Phys.* **55**, 1171 (1985)
  - [5] J.A.C. Veerman and D. Frenkel, *Phys. Rev. A* **45**, 5632 (1992)
  - [6] D. Frenkel, *Physica A* **263**, 26 (1999)
  - [7] S.-J. Marink and D.P. Tieleman, *J. Am. Chem. Soc.* **123**, 12383 (2001)
  - [8] S.-J. Marink and D.P. Tieleman, *Biophys. J.* **83**, 2386 (2002)
  - [9] J. Harting, J. Chin, M. Venturoli and P.V. Coveney, *Phil. Trans. R. Soc. A* **363**, 1895 (2005)
  - [10] F. Barmes, M. Ricci, C. Zannoni and D.J. Cleaver, *Phys. Rev. E* **68**, 021708 (2003)
  - [11] J.M. Seddon and R.H. Templer, *Phil. Trans. R. Soc. A* **344**, 377 (1993)
  - [12] A.H. Schoen, *NASA Technical Note D-5541*, Washington DC (1970)
  - [13] M. Impérator-Clerc, *Curr. Op. Coll. Int. Sci.* **9**, 370 (2005)
  - [14] D. Fazio, C. Mongin, B. Donnio, Y. Galerne, D. Guillon and D.W. Bruce, *J. Mater. Chem.* **11**, 2852 (2001)
  - [15] X.B. Zeng, G. Ungar and M. Impérator-Clerc, *Nature Materials* **4**, 562 (2005)
  - [16] U. Seifert, K. Berndl and R. Lipowsky, *Phys. Rev. A* **44**, 1182 (1991)
  - [17] W.K. Kegel, D. Breed, M. Elsesser and D.J. Pine, *Langmuir* **22**, 7135 (2006)
  - [18] A.M. Squires, R.H. Templer, J.M. Seddon, J. Woenkhaus, R. Winter, S. Finet and N. Theyencheri, *Langmuir* **18**, 7384 (2002)
  - [19] M. Clerc, A.M. Levelut and J.F. Sadoc, *Journal de Physique II*, **1**, 1263(1991)

FIG. 1: (a) configuration snapshot of an Ia3d structure formed by  $k = 3$ ,  $k_\theta = 3.8$  tapered particles. Each tapered particle has a light pointed end and a darker blunt end. (b) wireframe representation of the two interpenetrating 3d networks (arbitrarily shown in different shades (colours on-line)) found in the configuration shown in (a) on performing cluster analysis on the blunt ends of the individual tapered particles. Inset: profile of an individual  $k = 3$ ,  $k_\theta = 3.8$  tapered particle.

FIG. 2: Wireframe snapshots depicting the locations of particle blunt ends at various time points following expansion of an initial smectic A bilayer arrangement. These are shown for timesteps 100,000 (a), 200,000 (b), 400,000 (c) and 800,000 (d). The original multi-planar topology develops holes (a) through which stalks grow (b,c) and adapt until the planes become highly fragmented and interconnected (d). Shades (colours on-line) indicate the planes with which the particle ends were associated at the beginning of the run.

FIG. 3: 2d particle-resolution schematics showing the configurations adopted to achieve (a) hole formation and (b) stalk formation, corresponding to features apparent from the wireframe snapshots shown in Figs 2a and 2b, respectively.

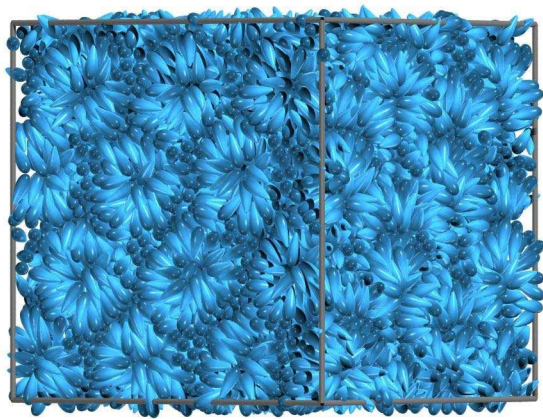


Figure 1a

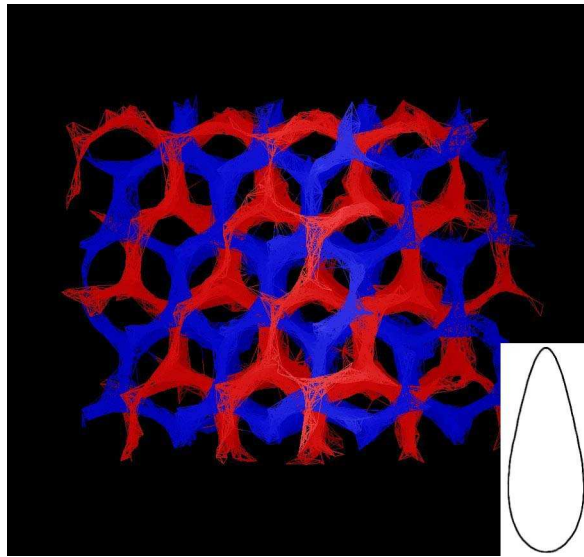


Figure 1b



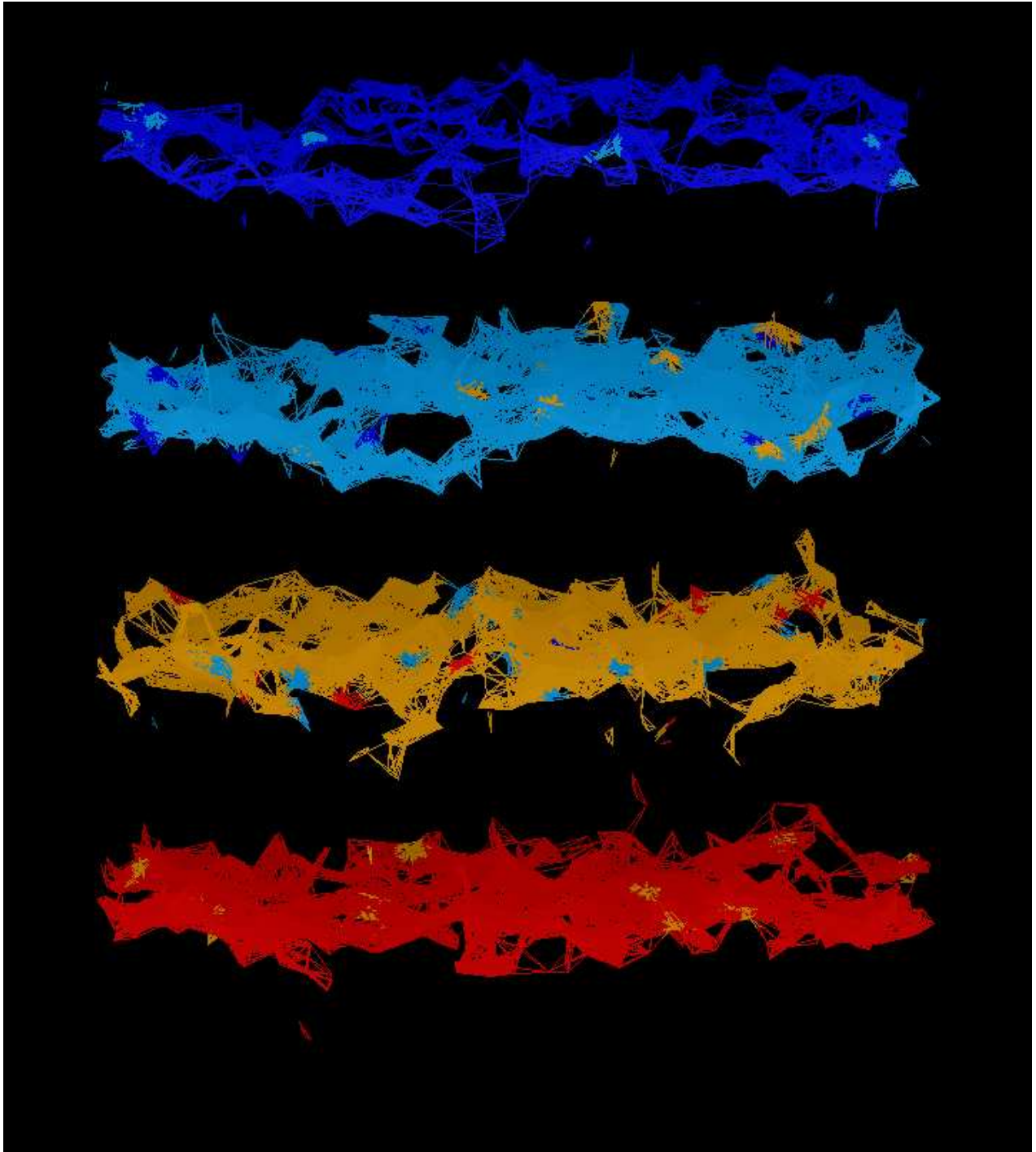


Figure 2a

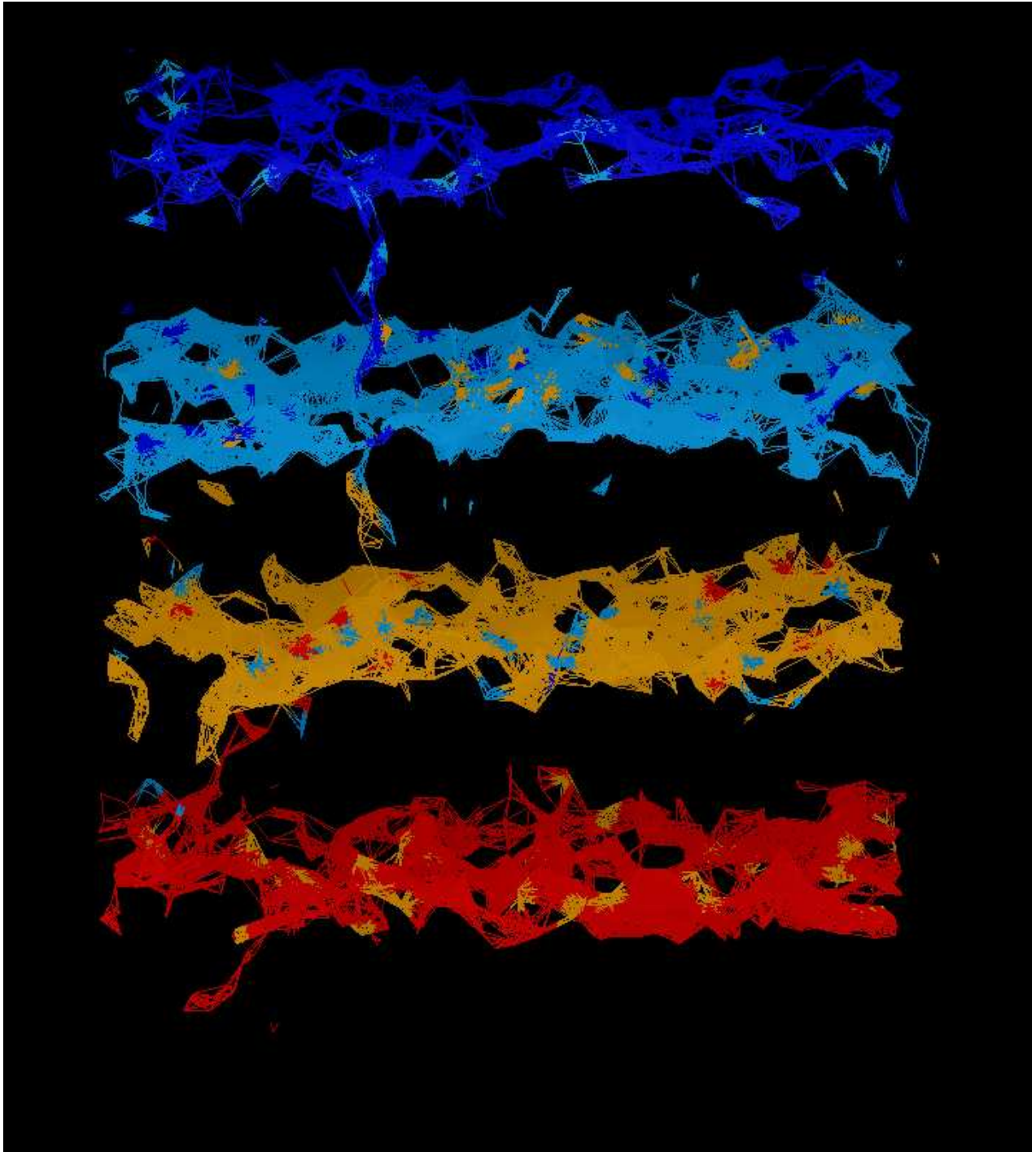


Figure 2b

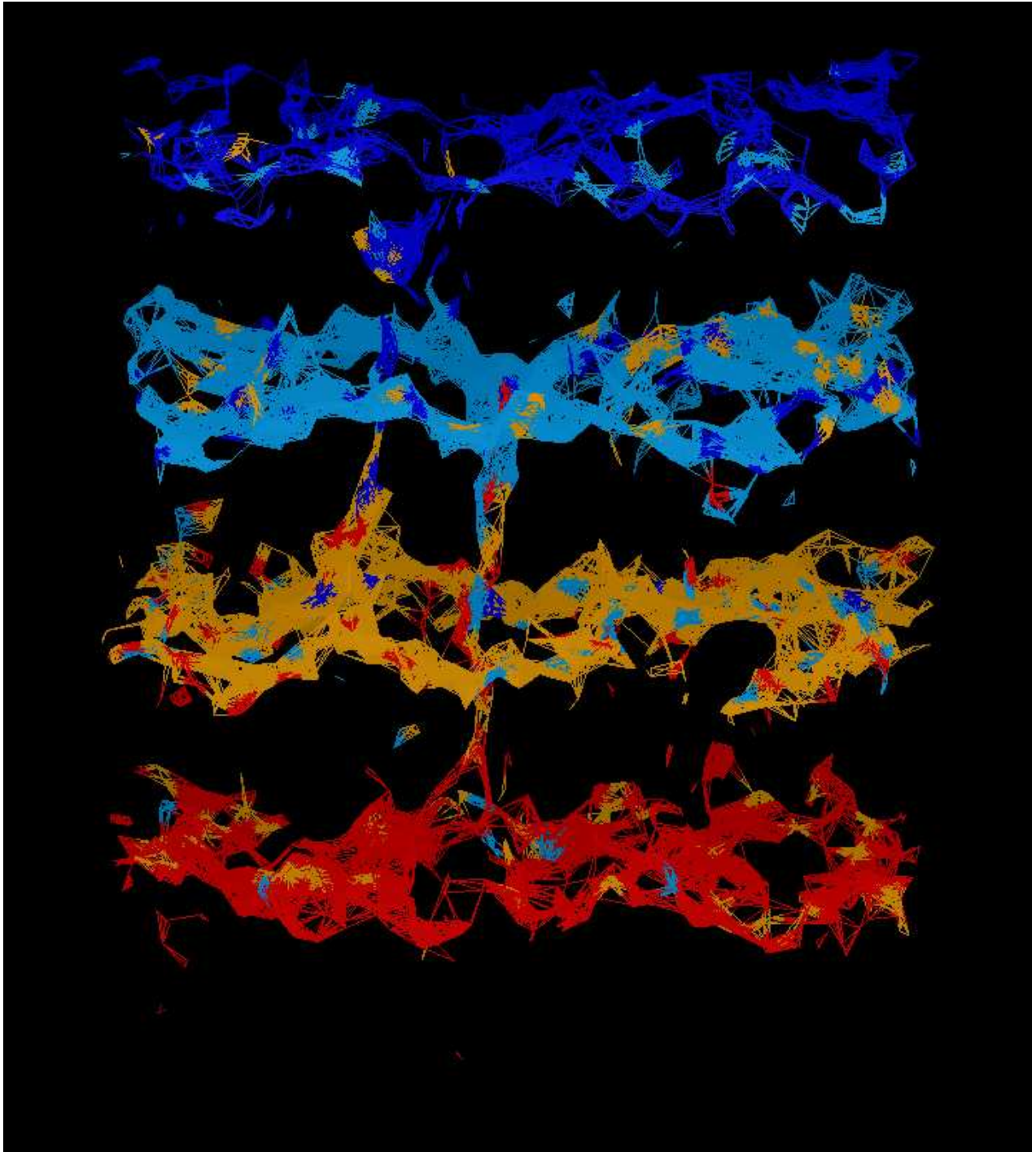


Figure 2c

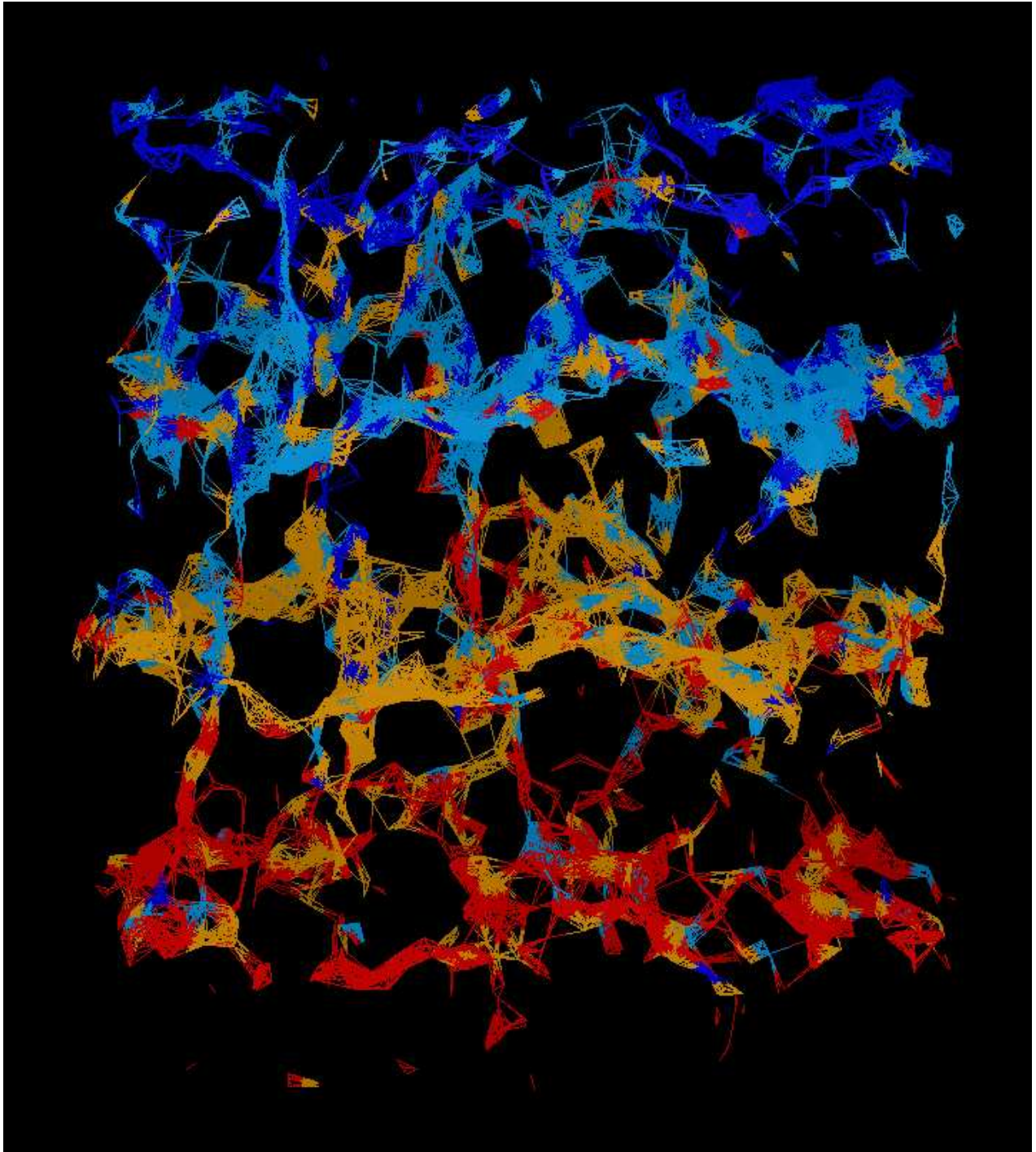


Figure 2d

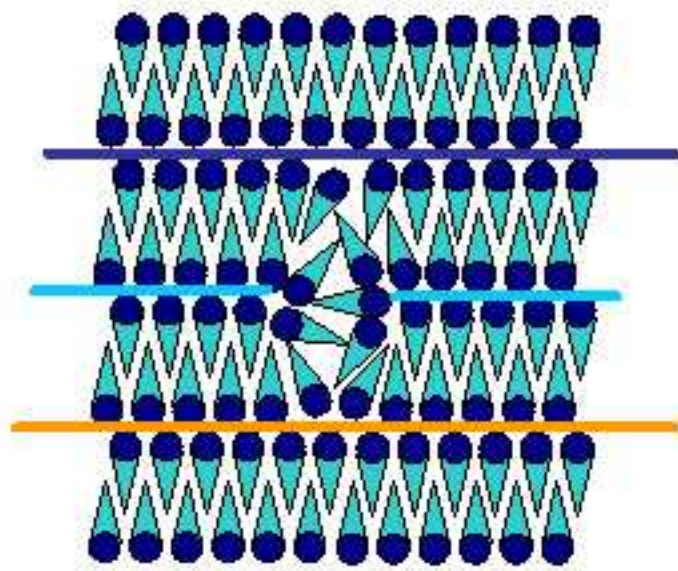


Figure 3a

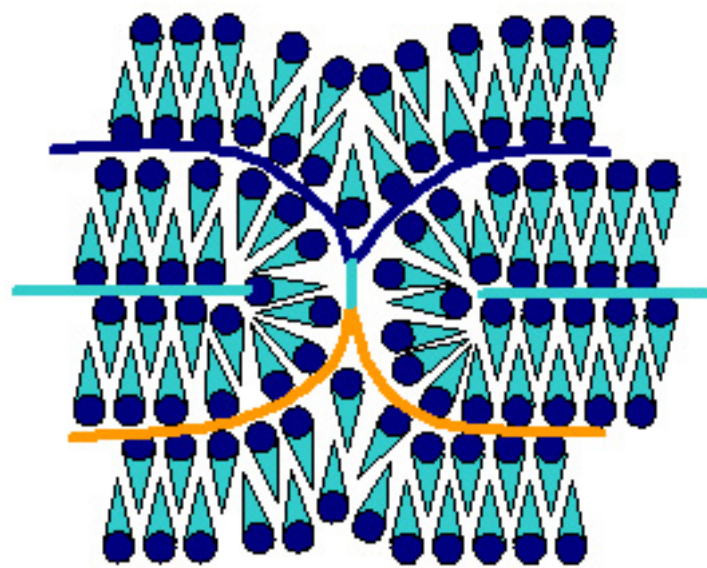


Figure 3b